

A numerical analysis of compressive strength of rectangular concrete columns confined by FRP

Huei-Jeng Lin[†], Chin-I Liao and Chin Yang

*Department of Engineering Science and Ocean Engineering National Taiwan University,
No. 1, Sec. 4, Roosevelt Road, Taipei 106, Taiwan*

(Received July 1, 2005, Accepted July 3, 2006)

Abstract. This investigation presents an analysis procedure for simulating the compressive behavior of a rectangular concrete column confined by fiber-reinforced plastic (FRP) under uniaxial load. That is, the entire stress-strain curve can be drawn through the present analysis procedure. The modified Mander's stress-strain model (Mander, *et al.* 1988) and finite element method are adopted in this analysis procedure. The numerical analysis results are compared with the experimental results to verify the accuracy of the analysis procedure. This study offers a useful analysis procedure of researching the compressive behavior of rectangular concrete columns confined by FRP. Two main parameters, the number of FRP layers and the radius of the round corners of a rectangular column, are investigated. The numerical results show that non-uniform stresses occur and reduce the sectional effective area owing to the geometry of the confined rectangular column. The stresses are concentrated at the corners of the rectangular column. Compressive strength of a rectangular column increases greatly because the number of FRP layers increase. The maximum predicted compressive stress of the rectangular column has approximately 10% error as compared to the experimental results. Comparing the numerical and experimental results demonstrates that the accuracy of this analysis procedure is credible. Besides, the stress-strain curves of the R30 models, which are rectangular concrete column with large radius of round corners, are almost bilinear. This calculated results conform to the expectation and show the present analysis procedure are more suitable than Mander's model (1988) to analyze the compressive behavior of the rectangular concrete column confined by FRP.

Keywords: concrete; rectangular column; fiber reinforced plastic (FRP); reinforcement; confined; finite element method (FEM)

1. Introduction

Fiber reinforced plastic (FRP) is commonly widely used in the shipbuilding industry, air industry, automobile industry, and sporting goods, and so on. FRP is widely used because of its excellent mechanical properties which include lightness, high strength, toughness, cheapness, and convenient implementation, and so on. Therefore, concrete reinforced by FRP can improve the mechanical properties of concrete, and thus research on how to use FRP to reinforce concrete is extremely important in the field of concrete structure reinforcement.

To reinforce an old structure is more economical than to rebuild it in situations where existing buildings fall short of new regulations regarding earthquake resistance standards. Steel tubes and plates are used to confine concrete structures, but steel is heavy, expensive, and inconvenient to

[†] PhD. Corresponding Author, E-mail: hjlin@ntu.edu.tw

process and maintain. Consequently, FRP has been considered as a replacement for steel. Safety considerations make it essential that columns do not crack when a structure is subjected to major external force. Thus, columns are the most important part of a structure. Accordingly, this study focuses on rectangular concrete column confined by carbon fiber reinforced plastic (CFRP). Mechanical behavior differs markedly between circular column and rectangular column. The geometry of rectangular columns causes stress concentration to occur at their corners. This study simulated the compressive behavior of the rectangular concrete column confined by FRP.

Numerous previous investigations have examined concrete structure reinforcement methods. One of the main issues is the effective confining area (Mander, *et al.* 1988, Shamim, *et al.* 1980, 1982). The effective lateral confining stress depends on the effective confining area which is smaller than the total cross area. Other influences on the lateral confining stress include spacing of the lateral steel bars (Saatcioglu and Razvi 1992), ratio of the long side length to the short side length of the cross-section (Hoshikuma, *et al.* 1997), number of FRP layers (Mirmiran, *et al.* 1998), and radius of the round corners of the rectangular column (Rochette and Labossiere 2000, Pessiki, *et al.* 2000, Lam and Teng 2001, Saatcioglu and Razvi 1992). Numerical analysis includes several achievements (Liu and Foster 1998, 2000, Mirmiran, *et al.* 2000, Parin and Wang 2001), and the finite element method (FEM) is widely used for numerical analysis.

The present investigation designs a simple analysis procedure for simulating the compressive behavior of a rectangular concrete column confined by FRP under uniaxial load. The numerical analysis results are compared with the experimental results to verify the accuracy of this analysis procedure.

2. Experiments

To get the properties of the plain concrete, compressive tests of circular plain concrete column were performed. The dimensions of the circular plain concrete column are ϕ 150×300 mm. The results are as the following. Compressive strength of the plain concrete is 21.09 MPa. Strain at the peak compressive stress is 0.0012. The Compressive modulus of elasticity is 21.12 GPa. Poisson's ratio is 0.2. Besides, the CFRP tensile tests were performed to obtain the material properties of the CFRP. Table 1 lists the results.

Nine sets of experiments were performed to get the compressive strength of the specimens. The dimensions of all specimens are 150×150×300 mm. The rule assigning numbers to the specimens is R#N#. The first symbol "#", including 0, 8, and 16, following the letter "R" indicates the radius of the round corner of the rectangular concrete column and its unit is mm. The second symbol "#",

Table 1 Material properties of the CFRP

σ_1^u	σ_2^u	ν_{12}
429.68 MPa	10.59 MPa	0.12
E_{11}	E_{22}	t
36.83 GPa	340 MPa	0.5 mm/ply
ϵ_1^u	ϵ_1^u	
1.5 %	3.1 %	

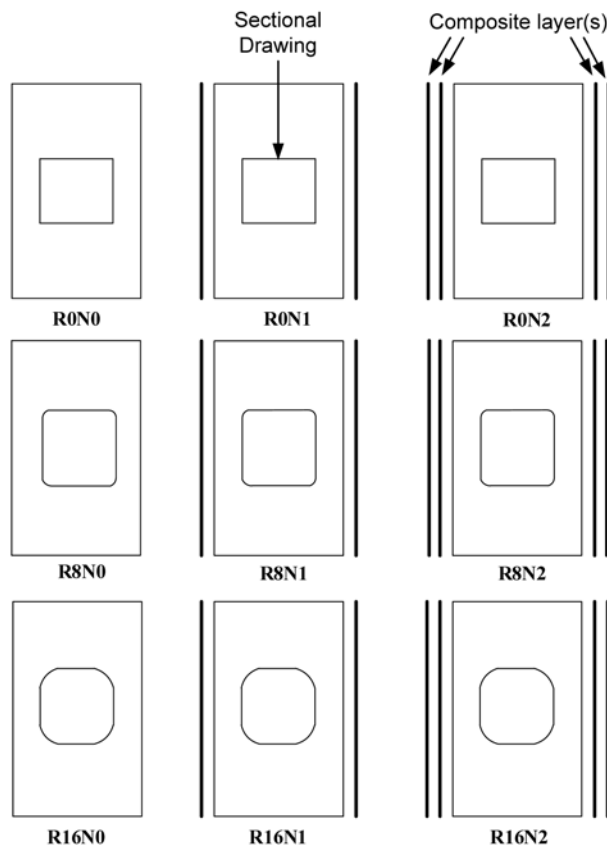


Fig. 1 Types of the FRP confinement for the every set of experiments

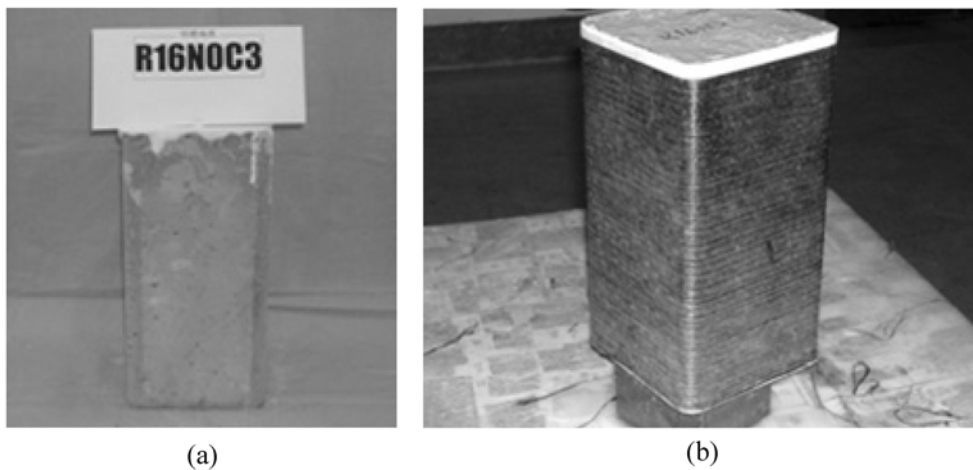


Fig. 2 (a) An unconfined rectangular concrete column (b) A rectangular concrete column confined with FRP

including 0, 1, and 2, following the letter “N” means the numbers of the FRP layers. Fig. 1 displays the types of the FRP confinement. Fig. 2 shows an unconfined rectangular concrete column and a

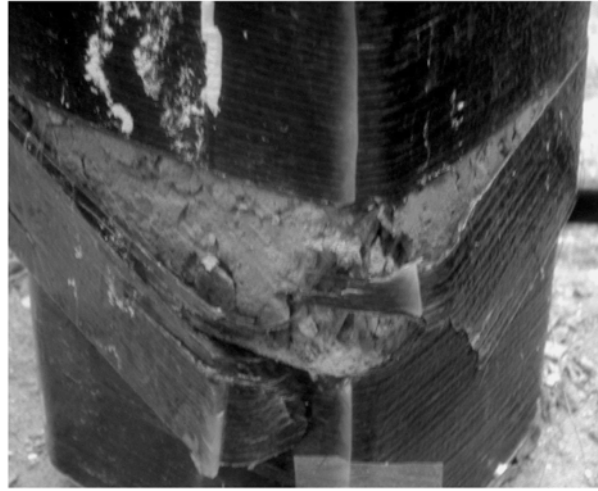


Fig. 3 CFRP often breaks from the middle corner of the rectangular concrete column

Table 2 Compression strength from the experimental results

Specimen No.	Stress (unit: MPa)								
	R0N0	R8N0	R16N0	R0N1	R8N1	R16N1	R0N2	R8N2	R16N2
1	18.15	19.13	19.62	26.19	26.19	29.04	28.74	30.12	failed
2	17.66	20.99	21.19	24.92	25.31	27.66	25.80	26.19	29.82
3	16.97	17.95	18.25	25.70	26.49	27.57	28.74	failed	30.51
Average	17.59	19.36	19.69	25.60	26.00	28.09	27.76	28.16	30.17

rectangular concrete column confined by FRP. CFRP often breaks from the middle corner of the rectangular concrete column and Fig. 3 shows the broken picture of a rectangular concrete column confined with CFRP.

Table 2 lists the compressive strength of the specimens from the experimental results, and some preliminary conclusions can be drawn. Firstly, the compressive strength increases with increasing the radius of the round corners of the rectangular concrete column, but its influence is indistinct because of the radius being too small. Second, the compressive strength increases with increasing number of CFRP layers which exert a distinct influence. What's more, the confining benefit of the CFRP is great despite the radius of the round corner being zero.

3. Analytical theory

Most predictions of the compressive strength of rectangular concrete column confined by FRP are obtained from regressive analysis, so they lack analytical theory. One reason why to use regressive analysis is the undetermined lateral confining stress applied by FRP. The influences on the lateral confining stress include stress concentration on corners, cross-section geometry, number of FRP layers, and radius of the round corners, and so on. This study synthesizes the stress-strain model of

Mander, *et al.* (1988), the shape factor of Lam and Teng (2001), and the commercial FEM software, ANSYS, to develop a procedure to analyze the rectangular concrete column confined by FRP. Mander, *et al.* (1988) demonstrated a mathematical model for fitting the stress-strain curve of a reinforced concrete column in 1988. This model is not only suitable for circular columns but also for rectangular columns. Many subsequent investigations were based on this model. Eqs. (1)~(5) show the equations used in Mander, *et al.* (1988) model.

$$f_c = \frac{f'_{cc} x^r}{r-1+x^r} \tag{1}$$

$$x = \frac{\epsilon_c}{\epsilon'_{cc}} \tag{2}$$

$$\epsilon'_{cc} = \epsilon'_{co} \left[1 + 5 \left(\frac{f'_{cc}}{f'_{co}} - 1 \right) \right] \tag{3}$$

$$r = \frac{E_{co}}{E_{co} - E_{sec}} \tag{4}$$

$$E_{sec} = \frac{f'_{cc}}{\epsilon'_{cc}} \tag{5}$$

The maximum axial compressive stress of the column f'_{cc} is the most important element in this model. Actually, the predictive method of f'_{cc} is always the key point in analyzing reinforced concrete column. Generally, f'_{cc} primarily depends on the lateral confining stress applied by confinement. Eqs. (6) and (7) are the equations for predicting f'_{cc} used in Mander, *et al.* (1988) model.

$$\frac{f'_{cc}}{f'_{co}} = -1.254 + 2.254 \sqrt{1 + 7.94 \frac{f'_l}{f'_{co}} - 2 \frac{f'_l}{f'_{co}}} \tag{6}$$

$$f'_l = k_e \times f_l \tag{7}$$

When a rectangular concrete column is confined by FRP, the lateral confining stress is not uniform. Because of the stress concentration, the confinement will lose its confining benefit. Mander, *et al.* (1988) used the effective confining coefficient (k_e) to modify the lateral confining stress for fitting this loss. Researchers had many different opinions regarding k_e . Among them, Pessiki, *et al.* (2000) thought k_e was primarily related to the cross-section geometry of the column. Pessiki, *et al.* (2000) recalled the effective confining coefficient (k_e) to shape factor (κ_s) and defined κ_s as Eq. (8). Pessiki, *et al.* (2000) suggested that the confinement is inefficient if κ_s is below 0.33, and is efficient if κ_s exceeds 0.5. Fig. 4 illustrates the effective area of a confined rectangular concrete column. The initial angle of the parabolic curve is assumed 45°.

$$\kappa_s = \frac{A_e}{A_{cc}} = 1 - \frac{\left[\frac{(h-2R)^2 + (b-2R)^2}{3hb} \right] - \rho_s}{1 - \rho_s} \tag{8}$$

After Pessiki, *et al.* (2000), Lam and Teng (2001) modified Pessiki's theory (2000) and defined

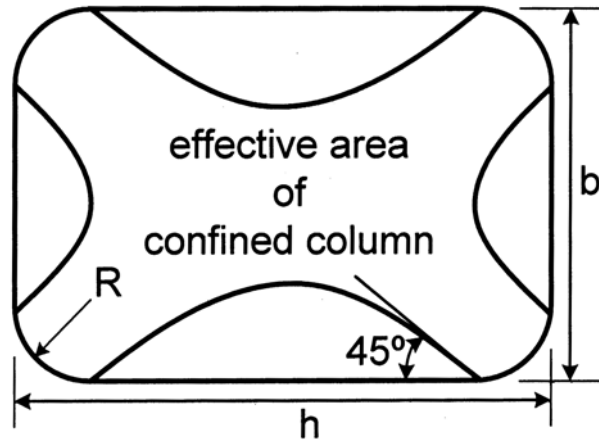


Fig. 4 Illustration of the effective area of confined rectangular concrete column

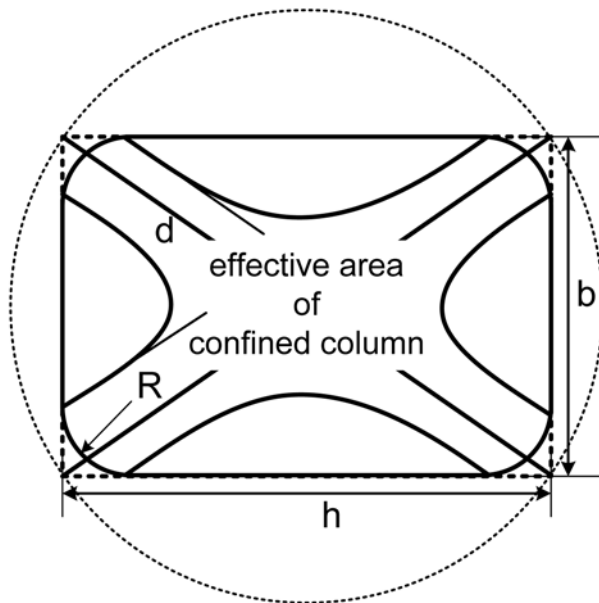


Fig. 5 Illustration of the effective area of confined rectangular concrete column.

Eqs. (9)~(12) for the shape factor (κ_s) in analyzing rectangular concrete columns confined by FRP. The difference from Pessiki's (2000) investigation, Teng's (2001) κ_s is calculated by defining equivalent circular column diameter (Eq. 12) and aspect ratio of the cross-section (b/h). Thus a method to analyze a confined circular column can be used to analyze a confined rectangular column through replacing the diameter with the length of the diagonal line of the rectangular cross-section. Fig. 5 illustrates the effective area of a confined rectangular concrete column. The difference from Fig. 4 is that the tangent line at the initial point of the parabolic curve is parallel to the diagonal line of the rectangular cross-section.

$$\kappa_s = \frac{bA_e}{hA_c} \tag{9}$$

$$\frac{A_e}{A_{cc}} = \frac{1 - \left[\frac{\frac{b}{h}(h-2R)^2 + \frac{h}{b}(b-2R)^2}{3A_b} \right] \rho_s}{1 - \rho_s} \tag{10}$$

$$A_g = bh - (4R^2 - \pi R^2) = bh - R^2(4 - \pi) \tag{11}$$

$$D = \sqrt{b^2 + h^2} \tag{12}$$

4. Numerical analysis procedure

The present analysis procedure uses the Mander’s model (1988), but replaces k_e in Eq. (7) with the shape factor k_s of Lam and Teng (2001) (in Eq. 10). The reason is that k_e is used in RC columns but k_s is taken into account for rectangular concrete columns confined by FRP. In Mander’s model (1988), the confining stress, f_i , has to be known first and then the stress-strain curve can be drawn. If the cross-section of the confined column is circular, the confining stress can be assumed uniform and calculated from force equilibrium. However, for a rectangular confined column, the confining stress is not uniform. So, this study uses the FEM commercial software, ANSYS, to calculate the distribution of the confining stress and take the maximum confining stress as f_i . During the process when a confined column is under compressive load, the compressed confined column deforms and expands more and more. So, the confining stress is larger and larger. When a strain of the confined column is given, the related confining stress distribution can be calculated through ANSYS and then a related longitudinal stress at the given strain can be got through Mander’s model (1988). Larger and Larger strains are given and every related longitudinal stresses are calculated through the above process. The stress-strain curve of a confined column under compressive load can be drawn. So, the present analysis procedure can be applied to simulate the compressive behavior of a rectangular concrete column confined by FRP under compressive load. That is, the entire stress-strain curve of a rectangular confined concrete column under compressive load can be drawn through the present analysis procedure.

Several assumptions are required to simplify the calculation. Plain concrete is a homogeneous material. The Poisson’s ratio of the plain concrete, ν_{co} , is 0.2. For the unidirectional CFRP, the 1-direction (fiber direction) is parallel to the fibers, and the 2-direction (transverse direction) is perpendicular to the fibers and lies in the plane of the lamina. 3-direction is the thickness direction. For circular cross-section fibers randomly distributed in a unidirectional lamina, the lamina can be further assumed macroscopically as transversely isotropic. So it was supposed tension modulus of the CFRP $E_1 \neq E_2 = E_3$, Poisson’s ratio $\nu_{12} = \nu_{13} = 0.12$, $\nu_{23} = 0.2$, shear modulus $G_{12} = G_{13}$, and $G_{23} = 0.01 G_{12}$ because of G_{23} is much smaller than G_{12} .

There are two parameters, the number of FRP layers and the radius of the round corners of a rectangular column, which will be studied through the present numerical analysis. Eight models were set up to study the influence of these two parameters on the compressive strength of rectangular concrete columns confined by CFRP. The dimensions of all models are 150×150×300

Table 3 Serial numbers and illustrations of all models

	R0N1	R0N2	R8N1	R8N2	R16N1	R16N2	R30N1	R30N2
R (mm)	0	0	8	8	16	16	30	30
N	1	2	1	2	1	2	1	2
t (mm)	0.5	1	0.5	1	0.5	1	0.5	1

The dimensions of all models are 150×150×300 mm.

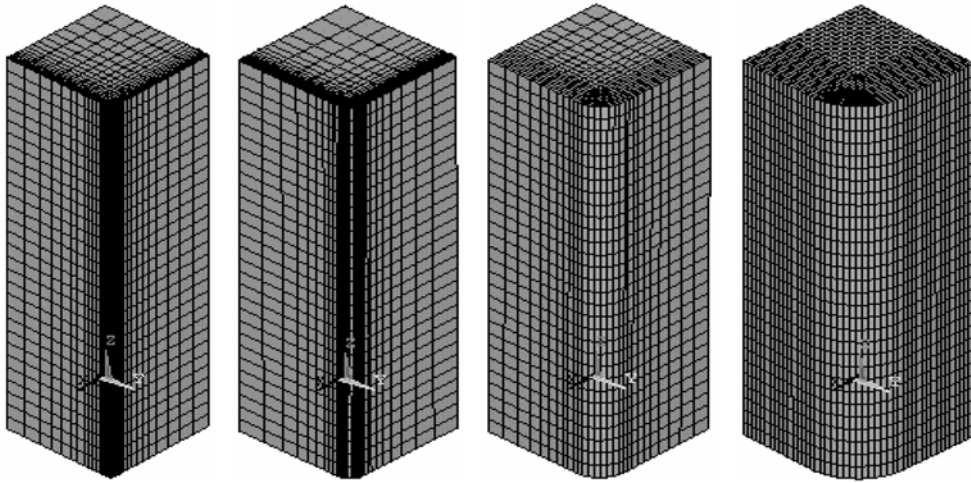


Fig. 6 The meshed models of R0, R8, R16, and R30

mm. The radius of the round corners of the first six models are the same as the experimental specimens. Notably, the radius of the round corners of the last two models is the same; it is 30 mm. Table 3 lists the serial numbers of the models. Mesh-sensitivity was checked by linear static analysis and the meshed models showed in Fig. 6 are the final version to be used. Symmetrical boundary conditions were used in order to minimize elements. Besides, refining mesh was used in the stress concentrating there. The element types used in ANSYS analysis are solid45 for concrete and shell63 for CFRP. The material properties of the CFRP and the concrete are mentioned above and in Table 1. If the material properties of plain concrete and CFRP are known, Mander's model (1988) only contains two variables, namely f'_c and ϵ_c . Accordingly, a f'_c can be found to yield a ϵ_c . The complete analysis procedure is presented as the following.

1. In the analysis procedure, the stress-strain diagram of CFRP is considered a straight line but that of the plain concrete is nonlinear. The way to deal with this problem is to use Mander's model (1988) with the condition $f'_l = 0$ to calculate the stress-strain diagram of the confined concrete core and use this calculated result to be the material properties of the plain concrete.
2. Input all material data of plain concrete and CFRP, which are got from the above experiment and the calculated results in step 1, into the FEM analysis software, ANSYS, and analyze the meshed model when a small axial strain is given. The distribution of the lateral confining stress applied by CFRP can be got.
3. Take the maximum lateral confining stress applied by CFRP, which is calculated in step 2, as

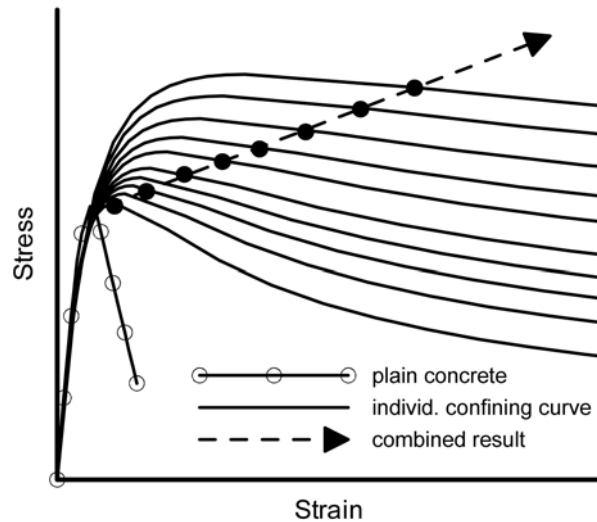


Fig. 7 The diagram of the present analysis procedure

f_i . Substitute f_i into Eq. (7) to calculate f'_i but replace k_c in Eq. (7) with the shape factor k_s in Eq. (10). That is, $f'_i = k_s \times f_i$, and let $\rho_s = 0$ since the core of the confined column is plain concrete. The longitudinal stress of the confined concrete column can be determined by using Mander's model (1988) (Eqs. 1~6). That is, the longitudinal stress, f_c , at the given axial strain, ϵ_c , can be calculated.

4. Give a small increment of axial strain and then recalculate the distribution of the lateral confining stress applied by CFRP by using the FEM analysis software, ANSYS.
5. Repeat steps 3 and 4 until the program terminates and the stress-strain diagram of the rectangular concrete column confined by CFRP under compressive load can be drawn. Because FRP is one kind of brittle materials, CFRP can be seen broken when the program terminates based on the condition that deformation of the element nodes are so large that the program diverges. The concrete column is also seen failed after the FRP is broken. Fig. 7 illustrates the diagram of the present analysis procedure.

5. Comparison between numerical and experimental results

When a concrete column confined by FRP is under compressive load, the concrete core will take almost loading in initial stage because the Poisson's ratio of concrete is very small and the deformation of the concrete core is small before the concrete core is damaged. Table 4 lists the numerical results and their errors related to the experimental results. Moreover, Figs. 8~10 show the comparisons of the stress-strain curves. All calculated curves approach experimental curves in the early stage in which the concrete core is still not fractured. Nevertheless, different trends occur after the concrete core cracked. The errors in Table 4 are the numerical results related to experimental results. The absolute values of the errors of the compressive strength are all around 10%. The absolute values of the strain errors are about 30%. The experimental strains represent the local strains since they are measured by strain gauges, but the numerical strains are determined based on

Table 4 Numerical results and errors related to experimental results

	f'_{cc}/f'_{co}			ϵ'_{cc}		
	Experimental	Numerical	Error (%)	Experimental	Numerical	Error (%)
R0N1	1.243	1.093	-12.07	0.00251	0.0018	-28.29
R0N2	1.348	1.153	-14.47	0.00313	0.0021	-32.91
R8N1	1.262	1.186	-6.02	0.00265	0.00182	-31.32
R8N2	1.367	1.381	1.4	0.00315	0.00273	-13.33
R16N1	1.362	1.251	-8.15	0.0031	0.003	-3.23
R16N2	1.467	1.627	10.91	0.00376	0.00515	36.97
R30N1	-	1.581	-	-	0.0108	-
R30N2	-	2.116	-	-	0.0116	-

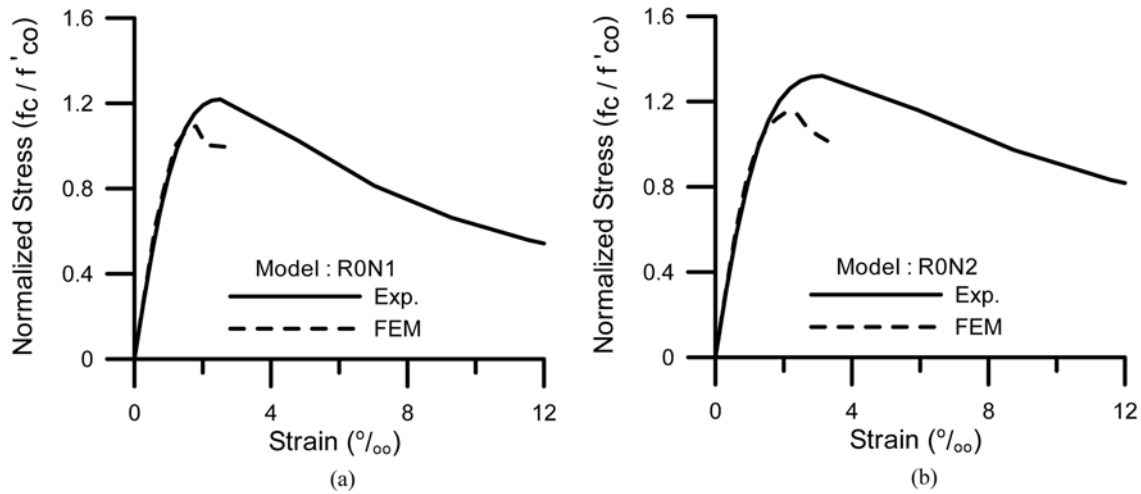


Fig. 8 Comparisons between numerical and experimental stress-strain curves of (a) R0N1 and (b) R0N2 models

the average strains. The fissures may be at, near, or far from the strain gauge so the measured strains differ significantly from the locations of the strain gauges when the concrete fractures. The above-mentioned is the main reason for the large errors of the strains. In general, the compressive strength is the most important factor in structural design. So, based on the facts that the calculated curves are close to experimental curves in the early stage and the errors of the compressive strength are small, the present analysis procedure is feasible to simulate the compressive behavior of the rectangular concrete column confined by CFRP. Moreover, Fig. 11 illustrates the distribution of the longitudinal stress on the cross-section of the R30 models. The stress concentrates on the four corners and the distribution area of the high stress resembles those in Fig. 4 and Fig. 5. From the above mentioned, the analytical results fit well with the results from experiments and in other investigations, so the correctness of the present analysis procedure is verified.

Pessiki, *et al.* (2000) suggested that the confinement is inefficient if κ_s is below 0.33, and is efficient if κ_s exceeds 0.5. For the present R30 models, κ_s is 0.76 so the confinement is efficient. That is, the compressive loading can be efficiently passed on CFRP. Therefore, the compressive

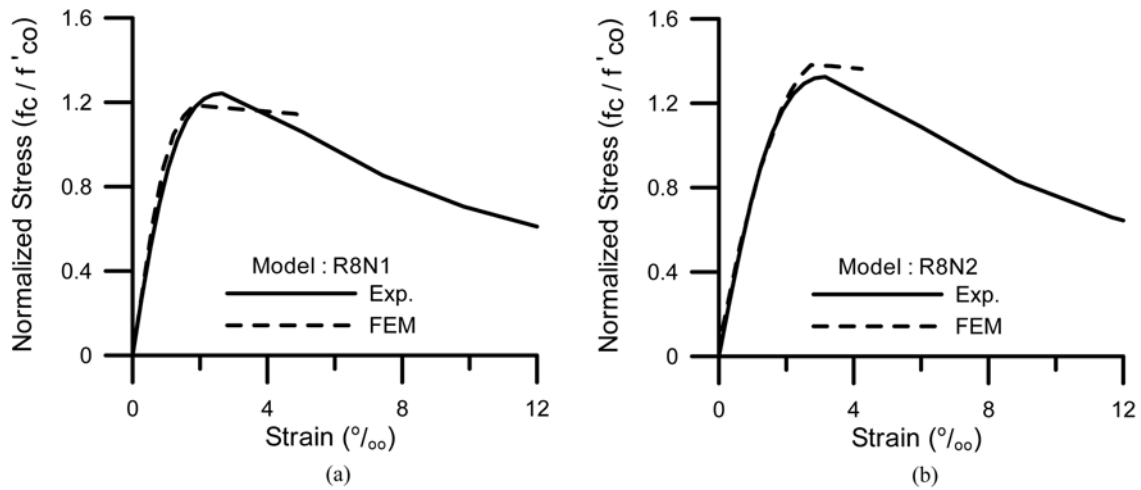


Fig. 9 Comparisons between numerical and experimental stress-strain curves of (a) R8N1 and (b) R8N2 models

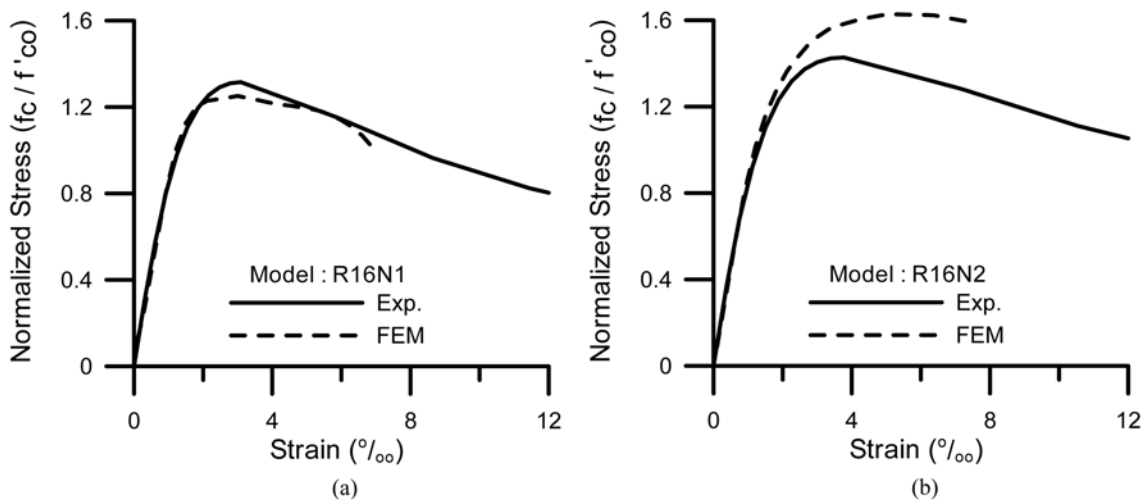


Fig. 10 Comparisons between numerical and experimental stress-strain curves of (a) R16N1 and (b) R16N2 models

behavior of the R30 models should be similar to that of the circular confined concrete column. From the author's previous study (Lin and Liao 2004), the stress-strain curves of a circular confined concrete column is bilinear and the stress-strain curves of the R30 models, which are showed by Fig. 12, are almost bilinear which conform to the expected circumstance. Furthermore, Fig. 12 also shows the stress-strain curves of the circular concrete column confined by 1-layer and 2-layer CFRP, which are calculated by Mander's model (1988). The compressive strength of R30N1 and R30N2 model are respectively a little lower than the compressive strength of the circular concrete column confined by 1-layer and 2-layer CFRP. This result is expectable because κ_s of the circular confined column is 1. However, the shortcoming of Mander's model (1988) is that the stress-strain

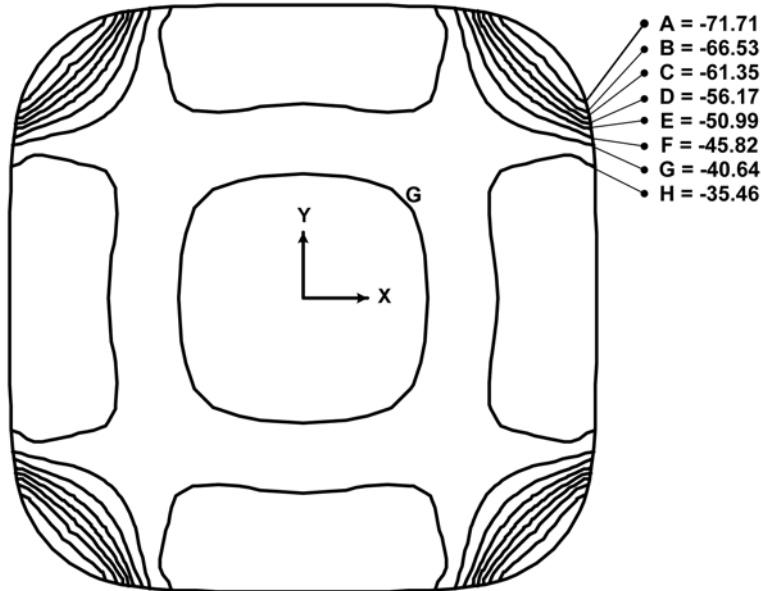


Fig. 11 Distribution of the axial compression stress, σ_x , on the cross-section of the R30N2 model (Unit: MPa)

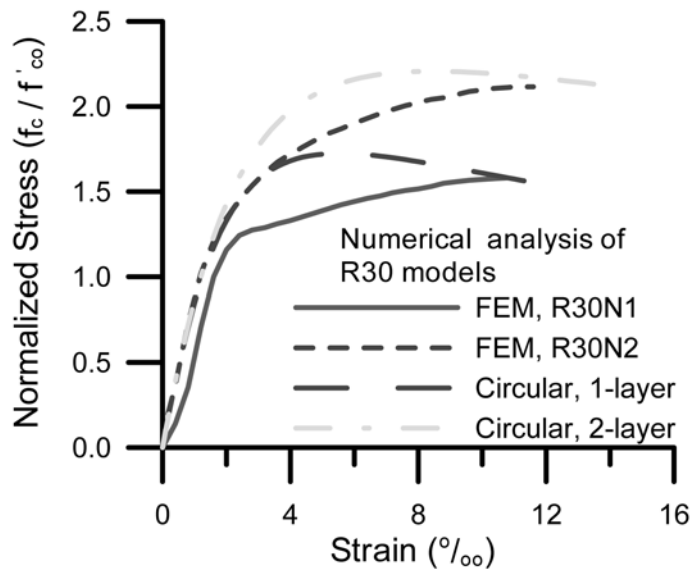


Fig. 12 Predicted stress-strain curves of the R30 models. “FEM” curves are calculated by the present analysis procedure, and “Circular” curves were directly calculated by Mander model (1988)

curves of circular concrete column confined by CFRP are not bilinear. That is not agreeable to the experiment results. Relatively, the present analysis procedure can improve this shortcoming.

6. Conclusions

This work presents a simple analysis procedure although the mechanical behavior of a confined rectangular concrete column is very complicated, and the following conclusions can be drawn. For a rectangular concrete column, the axial stress concentrates at the four corners so that almost all specimens crack from the corners. In the compressive process, the axial rigidity will reduce owing to the fractures of the concrete core, but does not drop abruptly because the concrete core is confined by FRP. The axial compressive strength greatly increases with increasing number of FRP layers. This tendency remains unchanged even though the radius of the round corner of the rectangular column is zero. However, for a rectangular concrete column with small radius of the round corners, the stress seriously concentrates at the corners and the concrete cracks here. After the concrete cracks at the corners, the lateral deformation at the corners increases rapidly. Therefore, the FRP is probably caused local breakage by cracked concrete and can not provide confining stress anymore. So, the effect of rectangular concrete column with large radius of the round corner confined by FRP is better than that of rectangular concrete column with small radius of the round corner confined by FRP. The axial compressive strength is increased greatly if the radius is sufficiently large, like the numerical model R30N1 or R30N2. For compressive strength of the rectangular concrete column confined by FRP, the errors of the numerical results related to the experimental results are all around 10%. Besides, from the comparison in Fig. 12, the stress-strain curves calculated through the present analysis procedure are close to bilinear, but those calculated through Mander's model (1988) are not bilinear. So, the present analysis procedure can simulate the compressive behavior of the rectangular concrete column confined by FRP better than Mander's model (1988). It can be demonstrated to be accurate and useful based on the discussion above.

Reference

- Hoshikuma, J., Kawashima, K., Nagaya, K. and Taylor, A.W. (1997), "Stress-strain model for confined reinforced concrete in bridge piers", *J. Struct. Eng.*, **123**(5), May, 624-633.
- Lam, L. and Teng, J.G. (2001), "Compressive strength of FRP-confined concrete in rectangular columns", *FRP Composites in Civil Engineering*, **1**, 335-342.
- Lin, Huei-Jeng and Liao, Chin-I (2004), "Compressive strength of reinforced concrete column confined by composite material", *Compo. Struct.*, **65**, pp. 239-250.
- Liu, Jing and Foster, Stephen J. (1998), "Finite-element model for confined concrete columns", *J. Struct. Eng.*, **124**(9), September, 1011-1017.
- Liu, Jing and Foster, Stephen J. (2000), "A three-dimensional finite element model for confined concrete structures", *Comput Struct.*, **77**(5), July, 441-451.
- Mander, J.B., Priestley, M.J.N. and Park, R. (1988), "Theoretical stress-strain model for confined concrete", *J. Struct. Eng.*, **114**(8), August, 1804-1826.
- Mirmiran, Amir, Shahaway, Mohsen, Samaan, Michel, El Echary, Hazem, Mastrapa, Juan Carlos and Pico, Odell (1998), "Effect of column parameters on FRP-Confined confined concrete", *J. Comp. Constr.*, **2**(4), November.
- Mirmiran, Amir, Zagers, Kenneth and Yuan, Wenqing (2000), "Nonlinear finite element modeling of concrete confined by fiber composites", *Finite Elements in Analysis and Design*, Elsevier, **35**(1), 9-96.
- Parin, Azadeh and Wang, Wei (2001), "Behavior of FRP jacketed concrete columns under eccentric loading", *J. Compo. Constr.*, **5**(3), August, 146-152.
- Pessiki, Stephen, Harries, Kent A., Kestner, Justin T., Sause, Richard and Ricles, James M. (2000), "Axial behavior of reinforced concrete columns confined with FRP jackets", *J. Comp. Constr.*, **4**(3), August, 237-245.

- Rochett, Pierre and Labossiere, Pierre (2000), "Axial testing of rectangular columns confined with composites", *J. Comp. Constr.*, **4**(3), August, 129-136.
- Saatcioglu, Murat, and Razvi, Salim R. (1992), "Strength and ductility of confined concrete", *J. Struct. Eng.*, **118**(6), June, 1590-1607.
- Shamim, A. Sheikh and Uzumeri, S.M. (1980), "Strength and ductility of tied concrete columns", *J. Struct. Div.*, **106**(ST5), May, 1079-1102.
- Shamim, A. Sheikh and Uzumeri, S.M. (1982), "Analytical model for concrete confinement in tied columns", *J. Struct. Div.*, **108**(ST12), December, 2703-2721.

Notation

The symbols used in this investigation are illustrated as follows.

- σ'_t : maximum tension stress
 E_t : tension modulus
 ε'_t : strain under
 f_c : axial compressive stress of the column
 ε_c : axial compressive strain of the column under f_c
 f'_{cc} : maximum axial compressive stress of the column
 ε'_{cc} : axial compressive strain of the column under f'_{cc}
 f'_{co} : compressive strength of the plain concrete
 ε'_{co} : compressive strain of the plain concrete under f'_{co}
 E_{co} : initial modulus of the plain concrete, which can be calculated by $E \cong 15964.27 \sqrt{f'_{co}}$ for MPa
 E_{sec} : secant modulus of the reinforced concrete column
 f'_l : effective lateral confining stress
 f_l : lateral confining stress
 f_j : tension strength of the composite layer(s)
 σ_1^u : ultimate stress parallel to the fiber direction
 σ_2^u : ultimate stress perpendicular to the fiber direction
 ε_1^u : strain parallel to the fiber direction under σ_1^u
 ε_2^u : strain perpendicular to the fiber direction under σ_2^u
 E_{11} : Young's modulus parallel to the fiber direction
 E_{22} : Young's modulus perpendicular to the fiber direction
 t_j : thickness of the composite layer(s)
 k_e : effective confining coefficient
 k_s : shape factor
 R : radius of the round corner of the rectangular concrete column
 N : number of the fiber layer(s)
 A_e : sectional effective area in the confined column
 A_{cc} : sectional area of concrete in the confined column
 ρ_s : sectional area ratio of axial steel to concrete in the confined column